LANGMUIR



Article

# Length-Dependent Diblock DNA with Poly-C as High Affinity Anchors on Graphene Oxide

Zhicheng Huang, and Juewen Liu

*Langmuir*, **Just Accepted Manuscript** • DOI: 10.1021/acs.langmuir.7b02812 • Publication Date (Web): 25 Sep 2017



ACS Publications

Langmuir is published by the American Chemical Society. 1155 Sixteenth Street N.W., Washington, DC 20036

# Length-Dependent Diblock DNA with Poly-C as High Affinity Anchors on Graphene Oxide

Zhicheng Huang and Juewen Liu*

Department of Chemistry, Waterloo Institute for Nanotechnology, University of Waterloo, Waterloo, Ontario, N2L 3G1, Canada

Email: liujw@uwaterloo.ca

The authors declare no conflict of interest.

**Abstract**

DNA-functionalized graphene oxide (GO) is a popular system for biosensor development and directed materials assembly. Compared to covalent attachment, simple physisorption of DNA has been more popular, and a DNA sequence with a strong affinity on GO is highly desirable. Recently, we found that poly-cytosine (C) DNA can strongly adsorb on many common nanomaterials, including GO. To identify an optimal length of poly-C DNA, we herein designed a series of diblock DNA sequences containing between 0 and 30 cytosines. The displacement of a random sequenced DNA by poly-C DNA was demonstrated, confirming the desired diblock structure on GO with the poly-C block anchoring on the surface and the other block available for hybridization. The adsorption density of poly-C containing DNA did not vary much as the length of the poly-C block increased, suggesting the conformation of the anchoring DNA on the GO was quite independent of the DNA length. With a longer poly-C block, the efficiency of surface hybridization of the other block increased, while non-specific adsorption of non-complementary DNA was inhibited more. Compared to poly-A containing DNAs, which were previously used for the same purpose, poly-C DNA adsorption is more stable. Using four kinds of 15-mer DNA homopolymers as the intended anchoring sequences, the $C_{15}$ DNA had the best hybridization efficiency. This work has suggested the optimal length for the poly-C block to be 15-mer or longer, and it has provided interesting insights into the DNA/GO biointerface.

## Introduction

DNA-functionalized nanomaterials have attracted extensive research interest,[1] allowing innovative applications in directed assembly,[2-5] biosensor development,[6-11] and drug or gene delivery.[12, 13] A key aspect is to attach DNA to nanomaterials to achieve stable and functional conjugates.[14] Covalent attachment, such as linking thiolated DNA to gold nanoparticles,[15-17] and $MoS_2$,[18, 19] and amino-modified DNA to graphene oxide (GO) is often carried out.[20, 21] Studying physisorption of DNA is also important for several reasons. First, the strength of physisorption determines the activity of DNA (e.g. for hybridization). If a DNA is adsorbed too strongly, it may lose its function of hybridization. For example, the DNA hybridization efficiency is very low if thiolated DNA is sparsely immobilized on a bare gold surface due to very strong nucleobase adsorption by gold.[22] Similarly, strong adsorption of DNA onto carbon nanotubes made DNA hybridization very slow.[23, 24] Second, physisorption may provide a cost-effective way for DNA conjugation. Taking advantage of the adsorption affinity difference between the four nucleobases, a few groups have developed methods to attach non-thiolated DNA to gold surfaces while still retaining the hybridization function of DNA.[25-27]

Similar to gold, GO is also a strong fluorescence quencher, while its DNA adsorption affinity is lower leading to more reversible DNA adsorption.[28-32] As such, GO has been a very popular platform for designing DNA-based biosensors.[33-36] At the individual nucleobase level, purines are adsorbed more tightly than pyrimidines.[37, 38] Thus, diblock poly-adenine (poly-A) containing DNA has been quite a popular choice to anchor on GO, with the other block intended for hybridization.[39, 40] We recently discovered that poly-C DNA is adsorbed even more tightly than poly-A DNA on most common inorganic surfaces including GO.[41] For the four types of 15-mer DNA homopolymers, $C_{15}$ more efficiently displaced the other sequences from GO, and $C_{15}$

was also the most resistant to displacement. This suggests that poly-C DNA may serve as an even better anchor than the commonly used poly-A DNA.

With this interesting observation, many questions remain to be addressed before we can take full advantage of the strong interaction between poly-C DNA and GO. The most important parameter is the length of the poly-C block. For example, it has been demonstrated that a longer poly-A sequence resulted in a lower DNA adsorption capacity on gold,[25, 26] indicating that the DNAs were arranged horizontally instead of in an upright conformation. On the other hand, poly-C DNA is prone to form the i-motif structure,[42] especially in the presence of nanosized carbons such as carbon nanotubes,[43, 44] fullerenes,[45] and graphene quantum dots.[46] Therefore, its packing on GO might be different from that of poly-A on gold. By systematically varying the length of poly-C DNA, and measuring its surface density and hybridization efficiency, we herein aim to better understand the adsorption mechanism for more efficient DNA immobilization and to identify the optimal DNA length.

## Materials and Methods

**Chemicals**. All the DNA samples were from Integrated DNA Technologies (IDT, Coralville, IA). Their sequences and modifications are listed in Table 1. Sodium chloride, magnesium chloride, and 4-(2-hydroxyethyl) piperazine-1-ethanesulfonate (HEPES) were from Mandel Scientific (Guelph, ON). Triton X-100, poly(acrylic acid) (PAA, MW: 15,000), poly(sodium 4-styrenesulfonate) (PSS, MW: 70,000), polyethylene glycol (PEG, MW: 20,000), dextran (MW: 500,000), bovine serum albumin (BSA), and fetal bovine serum (FBS) were from Sigma-Aldrich (St Louis, MO). Carboxyl graphene oxide (GO) was purchased from ACS Material (Medford, MA). Milli-Q water was used for all the experiments.

**Table 1.** DNA sequences and modifications used in this study.

| ID | DNA Name | Sequences 5′-3′ |
|---|---|---|
| **1** | 12mer ($C_0$-12mer) | TCACAGATGCGT |
| **2** | 12mer-c | ACGCATCTGTGA |
| **3** | $C_5$-12mer | TCACAGATGCGTCCCCC |
| **4** | $C_{10}$-12mer | TCACAGATGCGTCCCCCCCCCC |
| **5** | $C_{20}$-12mer | TCACAGATGCGTCCCCCCCCCCCCCCCCCCCC |
| **6** | $C_{30}$-12mer | TCACAGATGCGTCCCCCCCCCCCCCCCCCCCCCCCCCCCCCC |
| **7** | FAM-$C_{10}$-12mer | FAM-TCACAGATGCGTCCCCCCCCCC |
| **8** | FAM-$C_{20}$-12mer | FAM-TCACAGATGCGTCCCCCCCCCCCCCCCCCCCC |
| **9** | FAM-$C_{30}$-12mer | FAM-TCACAGATGCGTCCCCCCCCCCCCCCCCCCCCCCCCCCCCCC |
| **10** | FAM-$A_{10}$-12mer | FAM-TCACAGATGCGTAAAAAAAAAA |
| **11** | FAM-$A_{20}$-12mer | FAM-TCACAGATGCGTAAAAAAAAAAAAAAAAAAAA |
| **12** | FAM-$A_{30}$-12mer | FAM-TCACAGATGCGTAAAAAAAAAAAAAAAAAAAAAAAAAAAA |
| **13** | $C_{15}$-12mer | TCACAGATGCGTCCCCCCCCCCCCCCC |
| **14** | $T_{15}$-12mer | TCACAGATGCGTTTTTTTTTTTTTTT |
| **15** | $A_{15}$-12mer | TCACAGATGCGTAAAAAAAAAAAAAAA |
| **16** | $G_{15}$-12mer | TCACAGATGCGTGGGGGGGGGGGGGGG |
| **17** | FAM-cDNA | FAM-ACGCATCTGTGA |
| **18** | FAM-rDNA | FAM-AGAGAACCTGGG |
| **19** | FAM-12mer | FAM-TCACAGATGCGT |
| **20** | $A_5$ | AAAAA |
| **21** | $A_{10}$ | AAAAAAAAAA |
| **22** | $A_{30}$ | AAAAAAAAAAAAAAAAAAAAAAAAAAAAAA |
| **23** | $C_5$ | CCCCC |
| **24** | $C_{10}$ | CCCCCCCCCC |
| **25** | $C_{30}$ | CCCCCCCCCCCCCCCCCCCCCCCCCCCCCC |

**Preparation of DNA/GO adsorption complex.**

For DNA adsorption on GO, DNA was always used in excess. In a typical experiment, GO (400 μg/mL) was mixed with DNA (8 μM) in buffer A (150 mM NaCl, 1 mM $MgCl_2$, 25 mM HEPES, pH 7.5) with a final volume of 500 μL. Then, all DNA-GO samples were incubated at room temperature overnight. The DNA-GO conjugates were washed with buffer A 3 times under 8000 rpm for 6 min and the purified products were stored at 4 °C for use.

**DNA hybridization kinetics.**

To study DNA hybridization on the GO surface, non-FAM-labeled DNA was used and the DNA was pre-adsorbed on GO as described above. Before the hybridization reaction, all the DNA-GO conjugates were washed with buffer A to get rid of free DNA. The baseline fluorescence with 50 nM FAM-cDNA or FAM-rDNA in buffer A was monitored by a plate reader (SpectraMax M3) with excitation at 490 nm and emission at 520 nm. Then 10 μL of DNA-GO conjugates (400 μg/mL of GO) were added into each well, and the final concentration of DNA-GO conjugates was 40 μg/mL. All kinetics of fluorescent change were further monitored.

**DNA displacement by polymers and surfactants**

FAM-labelled poly-C and poly-A containing DNAs were first adsorbed onto GO. The stability of GO-DNA conjugates was studied with 90 μL of GO-DNA (20 μg/mL) in buffer A, and then 10 μL of different polymers/surfactants were added. The fluorescence of the sample with only 20 μg/mL of GO-DNA in buffer A (without added polymers or surfactants) was set as the background, which was used to calculate the percentage of DNA released. Surfactants such as Triton X-100 may cause bubbles, which need to be carefully removed to avoid artifacts. The

fluorescent intensity was measured by the plate reader (SpectraMax M3) with excitation at 490 nm and emission at 520 nm.

## Results and Discussion

**DNA length-dependent displacement reaction on GO.** Since our goal is to achieve specific DNA hybridization on GO, most of our DNA sequences contained two blocks. One block was a random 12-mer sequence intended for hybridization with its complementary target DNA. The other block was a poly-C sequence containing between 0 and 30 cytosine bases. For comparison, DNAs with a poly-A block were also used. We used poly-A (instead of poly-T or poly-G) here because poly-A had been the most popular anchoring sequence on GO.[36, 37] The reason for this diblock DNA design was based on the assumption that the poly-C block is adsorbed more strongly than the 12-mer random block. Therefore, at high DNA concentrations, all the DNAs are adsorbed via the poly-C block (e.g. the initially adsorbed random sequence is expected to be displaced by the higher affinity poly-C, Figure 1A). This DNA sequence-dependent displacement reaction has been demonstrated on AuNPs.[25, 26, 47]

To confirm this displacement reaction on GO, we first adsorbed a FAM-labeled 12-mer random DNA as a probe on GO, resulting in quenched fluorescence. Then non-labeled $C_5$, $C_{10}$, $C_{30}$, $A_5$, $A_{10}$ and $A_{30}$ oligonucleotides were respectively added (just homo DNA sequences, not diblock), and the kinetics of fluorescence change were followed (Figure 1B). We also added the non-labeled 12-mer random DNA (named 12mer DNA) and its complementary DNA (12mer-cDNA) for comparison. The fastest fluorescence enhancement was observed with the 12mer-cDNA, and this is attributable to its formation of a duplex DNA with the adsorbed probe. DNA is adsorbed on GO via its bases, and the bases are hidden in the duplex. This reaction is also the basis of DNA detection using GO.[33-36] For the poly-C DNAs, the rate of fluorescence

enhancement increased as the DNA length increased (Figure 1C). With the longest $C_{30}$, the rate of probe desorption was comparable to that of the 12mer-cDNA. The signal from the $C_5$ DNA was similar to that from the 12-mer random sequence. Overall, a longer poly-C DNA was more efficient in displacing the random sequence, suggesting a stronger adsorption affinity on GO.

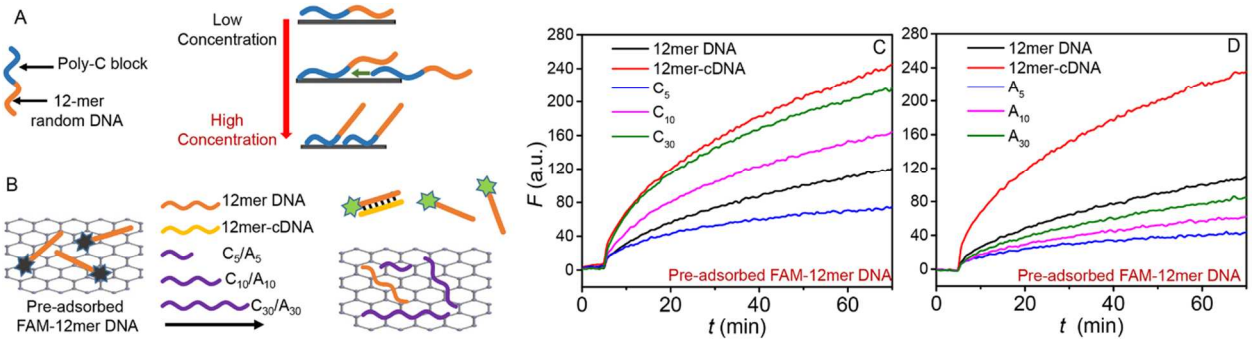


**Figure 1** (A) A scheme of a diblock DNA containing a poly-C block for adsorption on GO. With increasing DNA concentration, the poly-C block gradually displaces the other block, leading to the upright conformation of the other block. (B) A scheme of FAM-12mer DNA adsorbed on GO displaced by other DNA sequences, resulting in the fluorescence recovery. Among the added DNAs, its cDNA resulted in a duplex formation, while the other DNAs relied on simple displacement reactions. Kinetics of desorption of FAM-12mer DNA from GO by (C) poly-C DNA ($C_5$, $C_{10}$ and $C_{30}$); and (D) poly-A DNA ($A_5$, $A_{10}$ and $A_{30}$). Its cDNA and the same sequence but non-labeled DNA were also tested. The experiments were carried out with DNA/GO conjugates (20 μg/mL of GO) in buffer A (150 mM NaCl, 1 mM $MgCl_2$, 25 mM HEPES, pH 7.5).

The trend was, however, quite different for the poly-A DNA (Figure 1D). The desorption rates induced by $A_5$, $A_{10}$ and $A_{30}$ were even slower than that of the 12mer random DNA. This

indicated that not all of the adenines in the poly-A DNAs were adsorbed. Although adenine is adsorbed on graphene more strongly than cytosine at the individual base level, poly-A is prone to intramolecular stacking, which may compete with its adsorption on GO, and this has been supported by simulation studies.[48, 49] Based on this simple displacement experiment, we concluded that poly-C DNA can effectively serve as an anchoring block and displace random DNA sequences as shown in Figure 1A, while the ability of poly-A DNA for such displacement reactions is weaker.

**Length-dependent adsorption capacity of poly-C DNA.** After confirming the displacement reaction, we then measured the adsorption density of our diblock DNAs on GO. To push for a thermodynamic equilibrium, we incubated each DNA with GO overnight in a high salt buffer: buffer A (150 mM NaCl, 1 mM $MgCl_2$, 25 mM HEPES, pH 7.5). Since both DNA and GO are negatively charged, a high salt concentration favors DNA adsorption.[29, 31] The amount of the DNA used during the adsorption process was in excess. After incubation, we washed away the non-adsorbed free DNA, and the DNA remained on GO was quantified after releasing them from the surface using concentrated urea.[50]

We quantified the adsorption density of the DNA with various lengths of the poly-C or poly-A block (e.g. 0, 10, 20, and 30, Figure 2B). Note that the $C_0$ DNA contained only the random 12-mer sequence. The DNAs with a $C_{10}$ or $A_{10}$ block were both adsorbed with a comparable or even slightly higher density than the 12-mer random sequence. Note that the total DNA length of the $C_{10}$ or $A_{10}$ containing DNA was 22 nucleotides, almost double that of the 12-mer random DNA (e.g. the $C_0$ sample in Figure 2B). The fact that they were still adsorbed at a higher density strongly indicated that not all the bases were adsorbed in these diblock DNAs.

The adsorption densities were quite similar for the $C_{10}$ and $C_{20}$ containing DNAs, while that of the $C_{30}$ DNA was about 25% lower. Apparently, the density of DNA was not linearly inversed with the length of the poly-C block. It is likely that the poly-C block folded into certain secondary structures, likely related to the i-motif to be adsorbed, which has been conformed previously on many carbon surfaces, including graphene oxide.[41, 43-46] The footprints of the structures on GO are similar for $C_{10}$ and $C_{20}$-containing DNAs, while such structures do not need 30 cytosines. The extra cytosines in the $C_{30}$ containing DNA may occupy additional space to slightly reduce the density. This is schematically shown in Figure 2A.

The situation was different for the poly-A DNA, where a roughly linear decrease was observed. By increasing the poly-A length from 10 to 20 adenines, however, did not reduce the adsorption density by 50% (only dropped 18%). On AuNPs, the density was inversely proportional to the length of the poly-A block.[25, 26] We reason that instead of each adenine base being adsorbed on GO, the conformation was more complex, and the final adsorption depended also on intramolecular interactions (e.g. base stacking and hydrogen bonding). Due to the relatively low affinity of the poly-A DNA based on the above displacement reaction, adsorption via the random block likely took place as well. It should be noted that the affinity of DNA adsorption on GO is much weaker as compared to that on gold.[15] As a result, the DNA base hydrogen bonding and stacking interactions can influence DNA adsorption on GO, but much less so on AuNPs.

Overall, this DNA-length-dependent density measurement has provided important information regarding the conformation of such diblock DNA on GO. It is likely that the poly-C containing DNAs were adsorbed via the poly-C block, while the poly-A block containing DNAs might have a less defined adsorption structure (Figure 2A). This also confirms that poly-C is

adsorbed more strongly than poly-A. The strong adsorption of poly-C should allow efficient hybridization of the other block, which was the intended design.

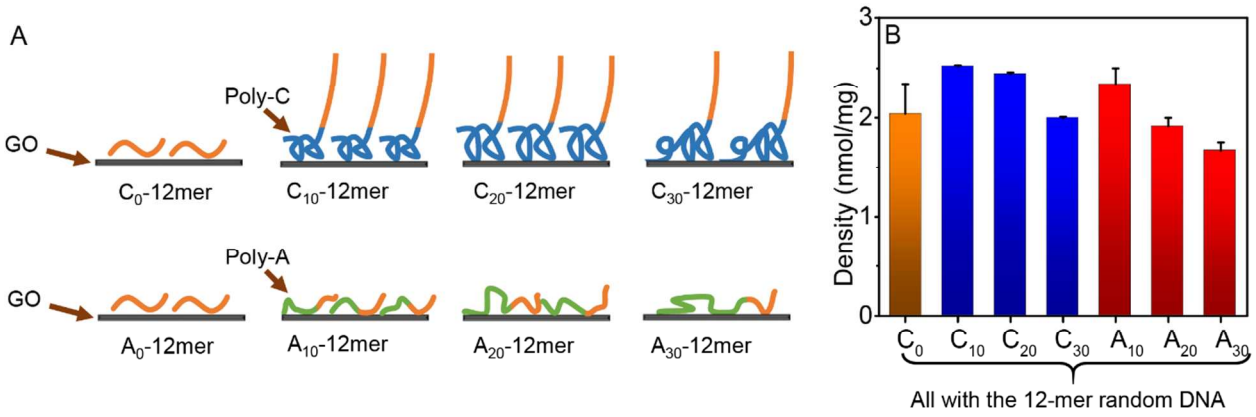


**Figure 2.** (A) A scheme showing the difference between poly-A and poly-C containing diblock DNA adsorption on GO (with excess DNA added). The panels on the left has only the random block. Poly-C containing DNAs are adsorbed via the poly-C block, while the poly-A containing DNAs are adsorbed more randomly. The poly-A block and the random block can both adsorb, but in each block not all the bases are adsorbed. (B) DNA adsorption density of the poly-C and poly-A containing DNAs with different lengths on GO (20 μg/mL).

**Poly-C length dependent DNA hybridization on GO**. The above adsorption capacity measurement suggested that the poly-C block was adsorbed on GO, exposing the other block for hybridization. This conformation was ideal for the intended DNA hybridization, and we aimed to obtain the optimal length of the poly-C block. It is likely that a DNA can be more stably adsorbed on GO with a longer poly-C block. However, when the poly-C is too long, the DNA

density decreases as demonstrated above, and the cost of DNA synthesis increases. Therefore, there might be an optimal length for poly-C.

To test this, we adsorbed a series of diblock DNAs on GO, each containing the same 12-mer random sequence but different lengths of the poly-C block. This is different from the above adsorption capacity measurement, as here the adsorbed DNAs were not labeled with a fluorophore. After removing the non-adsorbed DNA, the samples were added to the FAM-12mer DNA complementary to the immobilized random block. An obvious fluorescence quenching was observed upon mixing in most of the samples (Figure 3A). With a longer poly-C, more fluorescence quenching was observed. The extent of quenching is related to the average distance between the fluorophore and the GO surface.

Such fluorescence quenching could be attributed to one or both of the following events. 1) The intended hybridization would bring the FAM group close to the GO surface and thus induce fluorescence quenching. 2) The FAM-12mer DNA might be directly adsorbed on the GO surface (by either adsorbing on the empty space or by displacing the already adsorbed DNA), also resulting in quenched fluorescence. With these in mind, we now discuss the kinetic trace of each DNA.

First, the DNA without any poly-C sequences could hybridize with the added FAM-cDNA (black trace, Figure 3A). Since there was no poly-C block, the hybridization product was a full duplex and it could not be adsorbed on the GO surface, leading to very little final fluorescence quenching (see Figure 3B for the reaction scheme). With longer poly-C anchors, more fluorescence quenching was observed, suggesting that more FAM-12mer DNA remained on the surface after hybridization (Figure 3C). This was consistent with a more stable anchoring effect of DNA with a longer poly-C block.

For comparison, we also added a 12mer random DNA (named FAM-rDNA), which could not hybridize with the poly-C containing DNA on GO. In this case, very interestingly, the trend was the exact opposite, where the strongest quenching was observed for the DNA without the poly-C block (black trace, Figure 3D). A weaker quenching was observed with a longer poly-C block. From $C_{15}$-12mer to $C_{30}$-12mer, no further improvement was observed. We explained this trend as follows. The $C_0$-12mer sample (without poly-C block) was adsorbed the weakest, and it was easily displaced by the added FAM-rDNA, leading to the best quenching (Figure 3E). For the sequences with longer poly-C blocks, they adsorbed stronger to better block the surface of GO, leading to less adsorption of the non-complementary FAM-DNA (Figure 3F).

This set of hybridization experiments further confirmed the anchoring role of the poly-C sequence, which supported specific hybridization of the other block and resisted non-specific hybridization or adsorption of non-complementary DNA. To better achieve this role, a poly-C DNA length of around 15-mer or longer appears to be the most effective.

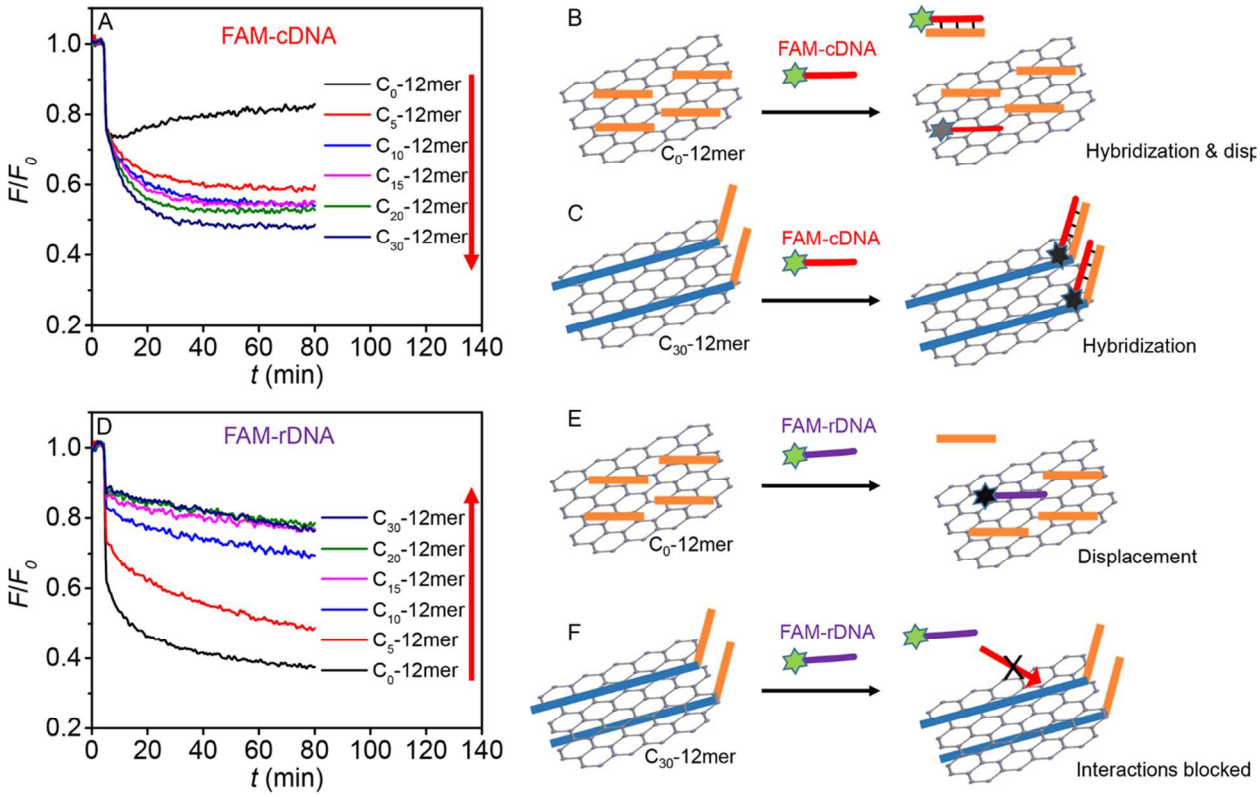


**Figure 3** (A) Kinetics of fluorescence drop after adding FAM-cDNA (FAM-labeled complementary DNA) to GO with pre-adsorbed DNA containing various lengths of poly-C. Proposed interactions between the added FAM-cDNA with GO pre-adsorbed with (B) DNA without a poly-C block and (C) the DNA with a long $C_{30}$ block. (D) Kinetics of fluorescence drop after adding FAM-rDNA (i.e. FAM-labeled random non-complementary DNA) to GO with pre-adsorbed DNA containing various lengths of poly-C. Proposed interactions between the added FAM-rDNA with GO pre-adsorbed with (E) DNA without poly-C block and (F) the DNA with a long $C_{30}$ block.

**DNA adsorption stability**. To serve as a useful anchoring sequence, adsorption stability is very important. In particular, without a covalent linkage, anchoring DNAs are still susceptible to non-specific displacement by other molecules. To explore the optimal DNA length in this regard, we then designed a systematic study. We adsorbed a few FAM-labeled poly-C containing sequences on GO and then incubated the samples with various competing molecules such as BSA protein and Triton-X 100. The fraction of released DNA was calculated based on the fluorescent intensity after 1 h of incubation (Figure 4A). As expected, the fraction of desorbed DNA decreased with increasing lengths of poly-C DNA. In particular, the most significant change occurred by going from $C_0$ to $C_{10}$.

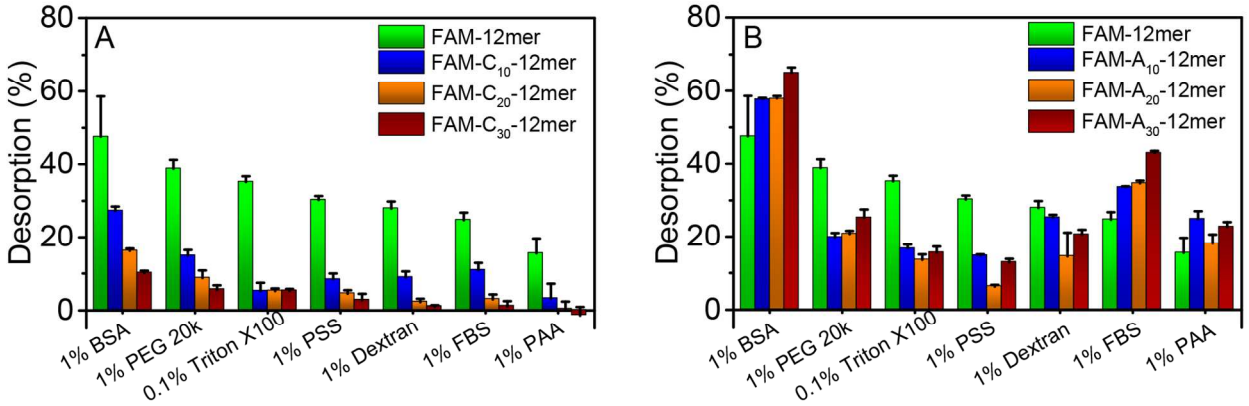


**Figure 4.** Percentage of desorption of the FAM-labeled (A) poly-C and (B) poly-A containing diblock DNA in the presence of various competing polymers and surfactants. A longer poly-C block was more resistant to desorption, while the effect of the length of the poly-A block was less obvious. The experiments were carried out in buffer A (150 mM NaCl, 1 mM $MgCl_2$, 25 mM HEPES, pH 7.5).

On the other hand, such a DNA length-dependent trend was not obvious for the poly-A containing sequences (Figure 4B). This poly-A experiment also served as a control to support the data of the poly-C containing DNA, and it was consistent with the previously observed weaker adsorption of the poly-A containing DNA. Given the adsorption density, hybridization kinetics, and adsorption stability data together, we reason that poly-C sequences of 15 nucleotides or longer are optimal for the anchoring purpose.

**Other anchoring sequences.** We mainly used poly-C and poly-A containing DNA to study DNA hybridization. To have a full understanding, we herein compared the four kinds of 15-mer DNA homopolymers, each containing a 12-mer random DNA intended for hybridization. Among them, the $C_{15}$ containing DNA still had the best hybridization performance, where 20% florescence quenching was observed with the FAM-cDNA (complementary DNA, black trace, Figure 5A). On the other hand, the fluorescence of the non-complementary DNA (FAM-rDNA, red trace, Figure 5A) barely changed, suggesting that the GO surface was effectively blocked. Both the $A_{15}$ and $T_{15}$ containing DNA had poor quenching selectivity for FAM-cDNA and FAM-rDNA (Figure 5B, 5C), suggesting such DNA design might not achieve the intended goal of specific hybridization on GO.

It was interesting to note that when the $G_{15}$ containing DNA was adsorbed on GO, approximately 33% florescence quenching of the FAM-cDNA was observed (note the initial ~10% drop due to the inner-filter effect of GO was not calculated), which appeared to be even better than the $C_{15}$ sample. Since poly-G DNA is known to quench fluorescence on its own (e.g. no need of GO), we then performed a control experiment of hybridizing the FAM-labeled DNA with the G15 containing DNA in the absence of GO. In this case, nearly 30% quenching was observed (Figure 5E). On the other hand, the other three DNA did not show such quenching

(Figure S1). Our previous studies also indicated that $G_{15}$ DNA was not stably adsorbed on GO.[41] Therefore, the drop in the $G_{15}$ containing sample cannot be attributed to the intended hybridization on the surface.

To have a better comparison, we plotted the difference between the black and red lines (e.g. the difference between the complementary and non-complementary DNA) in each experiment to represent specific hybridization (Figure 5F, green bars), where both $G_{15}$ and $C_{15}$ showed specific quenching suggesting hybridization took place for these two samples. For $A_{15}$, the cDNA sample had only a slight more fluorescence drop than the rDNA, while for the $T_{15}$ sample, barely any difference was observed. The red bars are quenching of the free DNA without GO. In this case, only the $G_{15}$ sample showed significant quenching. Comparing all the samples together, only the $C_{15}$ sample had a much higher green bar than the red bar, indicating it is the best candidate for anchoring on GO among these four sequences.

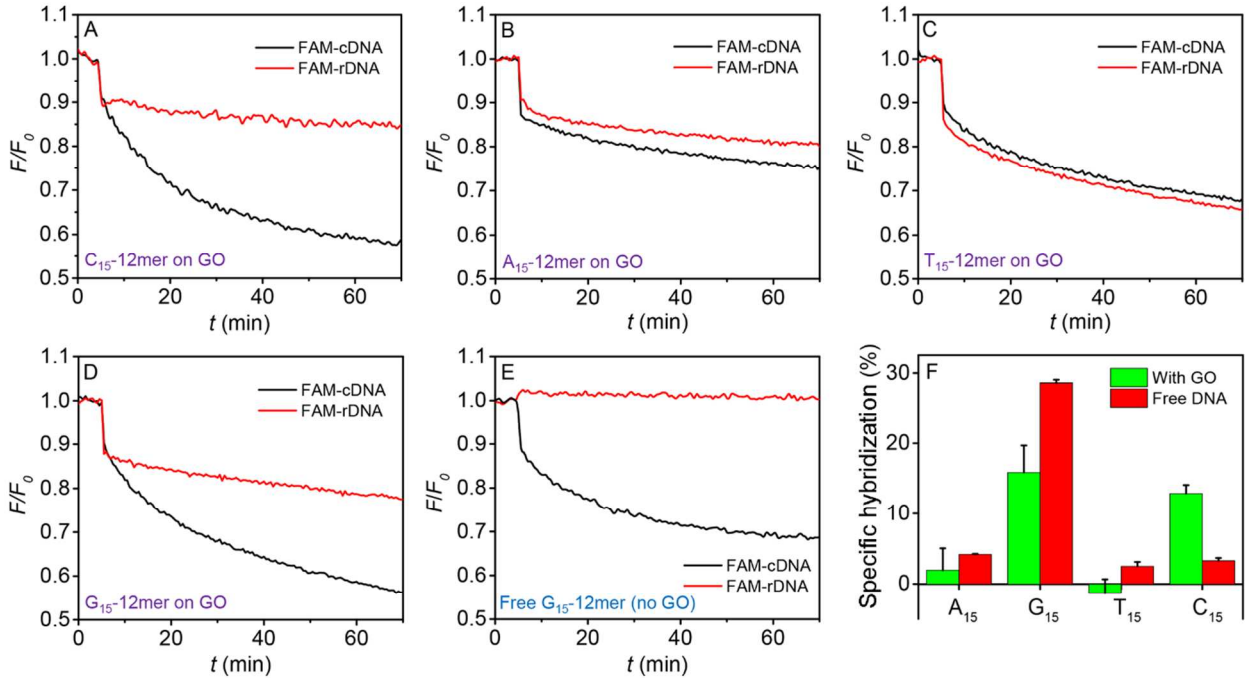


**Figure 5.** FAM-cDNA (specific hybridization) and FAM-rDNA (non-specific adsorption) kinetics on GO with four kinds of pre-adsorbed diblock DNA: (A) $C_{15}$-12mer DNA, (B) $A_{15}$-12mer DNA, (C) $T_{15}$-12mer DNA, and (D) $G_{15}$-12mer. (E) Fluorescence quenching induced by free $G_{15}$-12mer DNA hybridization. (F) Percentage of fluorescence qenching of FAM-cDNA with GO pre-adsorbed DNA (green bar) and free DNA (red bar) after subtracting the background of FAM-rDNA at 1 h.

## Conclusions

In summary, we conducted a systematic study of the length of poly-C DNA for adsorption on GO using a series of diblock DNAs, all containing the same 12-mer random sequence as a functional block for hybridization. In general, the poly-C block can effectively displace the random sequence from GO, thus confirming the intended adsorption conformation of DNA, where the poly-C block is anchored on the surface of GO while the other block is away

from GO and available for hybridization. Unlike adsorbing poly-A DNA on AuNPs, the adsorption density of poly-C DNA was not inversely linearly dependent on the length of the poly-C block. This is likely due to i-motif type of conformation of poly-C DNA on GO. With increasing poly-C length, specific hybridization on GO was promoted, while non-specific adsorption was inhibited, further confirming the model of poly-C blocking serving as an anchor. When challenged with various polymers and surfactants, the poly-C containing DNA showed length-dependent resistance to displacement, while the poly-A DNA did not have an obvious length effect. Our data is consistent with poly-C being adsorbed much more strongly on GO than poly-A or other DNA, and the optimal length of poly-C is determined to be 15-mer or longer.

**Acknowledgements**

Funding for this work is from the Canadian Foundation for Innovation, the Natural Sciences and Engineering Research Council (NSERC) of Canada.

**References**

(1) Cutler, J. I.; Auyeung, E.; Mirkin, C. A., Spherical Nucleic Acids. *J. Am. Chem. Soc.* **2012**, 134, 1376-1391.

(2) Jones, M. R.; Seeman, N. C.; Mirkin, C. A., Programmable Materials and the Nature of the DNA Bond. *Science* **2015**, 347, 1260901.

(3) Macfarlane, R. J.; Lee, B.; Jones, M. R.; Harris, N.; Schatz, G. C.; Mirkin, C. A., Nanoparticle Superlattice Engineering with DNA. *Science* **2011**, 334, 204-208.

(4) Nykypanchuk, D.; Maye, M. M.; van der Lelie, D.; Gang, O., DNA-Guided Crystallization of Colloidal Nanoparticles. *Nature* **2008**, 451, 549-552.

(5) Tan, L. H.; Xing, H.; Lu, Y., DNA as a Powerful Tool for Morphology Control, Spatial Positioning, and Dynamic Assembly of Nanoparticles. *Acc. Chem. Res.* **2014**, 47, 1881-1890.

(6) Rosi, N. L.; Mirkin, C. A., Nanostructures in Biodiagnostics. *Chem. Rev.* **2005**, 105, 1547-1562.

(7) Wang, H.; Yang, R. H.; Yang, L.; Tan, W. H., Nucleic Acid Conjugated Nanomaterials for Enhanced Molecular Recognition. *ACS Nano* **2009**, 3, 2451-2460.

(8) Liu, J.; Cao, Z.; Lu, Y., Functional Nucleic Acid Sensors. *Chem. Rev.* **2009**, 109, 1948–1998.

(9) Zhou, W.; Saran, R.; Liu, J., Metal Sensing by DNA. *Chem. Rev.* **2017**, 117, 8272–8325.

(10) Li, D.; Song, S. P.; Fan, C. H., Target-Responsive Structural Switching for Nucleic Acid-Based Sensors. *Acc. Chem. Res.* **2010**, 43, 631-641.

(11) Li, J.; Mo, L.; Lu, C.-H.; Fu, T.; Yang, H.-H.; Tan, W., Functional Nucleic Acid-Based Hydrogels for Bioanalytical and Biomedical Applications. *Chem. Soc. Rev.* **2016**, 45, 1410-1431.

(12) Pei, H.; Zuo, X. L.; Zhu, D.; Huang, Q.; Fan, C. H., Functional DNA Nanostructures for Theranostic Applications. *Acc. Chem. Res.* **2014**, 47, 550-559.

(13) Fan, H.; Zhang, X.; Lu, Y., Recent Advances in DNAzyme-Based Gene Silencing. *Sci. China Chem.* **2017**, 60, 591-601.

(14) Liu, B.; Liu, J., Methods for Preparing DNA-Functionalized Gold Nanoparticles, a Key Reagent of Bioanalytical Chemistry. *Anal. Methods* **2017**, 9, 2633-2643.

(15) Liu, J., Adsorption of DNA onto Gold Nanoparticles and Graphene Oxide: Surface Science and Applications. *Phys. Chem. Chem. Phys.* **2012**, 14, 10485-10496.

(16) Carnerero, J. M.; Jimenez-Ruiz, A.; Castillo, P. M.; Prado-Gotor, R., Covalent and Non-Covalent DNA–Gold-Nanoparticle Interactions: New Avenues of Research. *ChemPhysChem* **2017**, 18, 17-33.

(17) Liu, B.; Liu, J., Freezing Directed Construction of Bio/Nano Interfaces: Reagentless Conjugation, Denser Spherical Nucleic Acids, and Better Nanoflares. *J. Am. Chem. Soc.* **2017**, 139, 9471–9474.

(18) Liu, T.; Wang, C.; Gu, X.; Gong, H.; Cheng, L.; Shi, X. Z.; Feng, L. Z.; Sun, B. Q.; Liu, Z., Drug Delivery with Pegylated $MoS_2$ Nano-Sheets for Combined Photothermal and Chemotherapy of Cancer. *Adv. Mater.* **2014**, 26, 3433-3440.

(19) Li, B. L.; Setyawati, M. I.; Chen, L.; Xie, J.; Ariga, K.; Lim, C.-T.; Garaj, S.; Leong, D. T., Directing Assembly and Disassembly of 2D $MoS_2$ Nanosheets with DNA for Drug Delivery. *ACS Appl. Mater. Inter.* **2017**, 9, 15286-15296.

(20) Mohanty, N.; Berry, V., Graphene-Based Single-Bacterium Resolution Biodevice and DNA Transistor: Interfacing Graphene Derivatives with Nanoscale and Microscale Biocomponents. *Nano Lett.* **2008**, 8, 4469-4476.

(21) Huang, P.-J. J.; Liu, J., A Molecular Beacon Lighting up on Graphene Oxide. *Anal. Chem.* **2012**, 84, 4192-4198.

(22) Herne, T. M.; Tarlov, M. J., Characterization of DNA Probes Immobilized on Gold Surfaces. *J. Am. Chem. Soc.* **1997**, 119, 8916-8920.

(23) Jeng, E. S.; Moll, A. E.; Roy, A. C.; Gastala, J. B.; Strano, M. S., Detection of DNA Hybridization Using the near-Infrared Band-Gap Fluorescence of Single-Walled Carbon Nanotubes. *Nano Lett.* **2006**, 6, 371-375.

(24) Yang, R. H.; Jin, J. Y.; Chen, Y.; Shao, N.; Kang, H. Z.; Xiao, Z.; Tang, Z. W.; Wu, Y. R.; Zhu, Z.; Tan, W. H., Carbon Nanotube-Quenched Fluorescent Oligonucleotides: Probes That Fluoresce Upon Hybridization. *J. Am. Chem. Soc.* **2008**, 130, 8351-8358.

(25) Opdahl, A.; Petrovykh, D. Y.; Kimura-Suda, H.; Tarlov, M. J.; Whitman, L. J., Independent Control of Grafting Density and Conformation of Single-Stranded DNA Brushes. *Proc. Natl. Acad. Sci. U.S.A.* **2007**, 104, 9-14.

(26) Pei, H.; Li, F.; Wan, Y.; Wei, M.; Liu, H.; Su, Y.; Chen, N.; Huang, Q.; Fan, C., Designed Diblock Oligonucleotide for the Synthesis of Spatially Isolated and Highly Hybridizable Functionalization of DNA-Gold Nanoparticle Nanoconjugates. *J. Am. Chem. Soc.* **2012**, 134, 11876-11879.

(27) Zhang, X.; Liu, B.; Dave, N.; Servos, M. R.; Liu, J., Instantaneous Attachment of an Ultrahigh Density of Nonthiolated DNA to Gold Nanoparticles and Its Applications. *Langmuir* **2012**, 28, 17053-17060.

(28) Liu, B.; Salgado, S.; Maheshwari, V.; Liu, J., DNA Adsorbed on Graphene and Graphene Oxide: Fundamental Interactions, Desorption and Applications. *Curr. Opin. Coll. Interface Sci.* **2016**, 26, 41-49.

(29) Wu, M.; Kempaiah, R.; Huang, P.-J. J.; Maheshwari, V.; Liu, J., Adsorption and Desorption of DNA on Graphene Oxide Studied by Fluorescently Labeled Oligonucleotides. *Langmuir* **2011**, 27, 2731–2738.

(30) Lee, J.; Yim, Y.; Kim, S.; Choi, M.-H.; Choi, B.-S.; Lee, Y.; Min, D.-H., In-Depth Investigation of the Interaction between DNA and Nano-Sized Graphene Oxide. *Carbon* **2016**, 97, 92-98.

(31) Park, J. S.; Goo, N.-I.; Kim, D.-E., Mechanism of DNA Adsorption and Desorption on Graphene Oxide. *Langmuir* **2014**, 30, 12587-12595.

(32) Tang, Z. W.; Wu, H.; Cort, J. R.; Buchko, G. W.; Zhang, Y. Y.; Shao, Y. Y.; Aksay, I. A.; Liu, J.; Lin, Y. H., Constraint of DNA on Functionalized Graphene Improves Its Biostability and Specificity. *Small* **2010**, 6, 1205-1209.

(33) Lu, C. H.; Yang, H. H.; Zhu, C. L.; Chen, X.; Chen, G. N., A Graphene Platform for Sensing Biomolecules. *Angew. Chem. Int. Ed.* **2009**, 48, 4785-4787.

(34) Wang, Y.; Li, Z. H.; Hu, D. H.; Lin, C. T.; Li, J. H.; Lin, Y. H., Aptamer/Graphene Oxide Nanocomplex for in situ Molecular Probing in Living Cells. *J. Am. Chem. Soc.* **2010**, 132, 9274-9276.

(35) He, S. J.; Song, B.; Li, D.; Zhu, C. F.; Qi, W. P.; Wen, Y. Q.; Wang, L. H.; Song, S. P.; Fang, H. P.; Fan, C. H., A Graphene Nanoprobe for Rapid, Sensitive, and Multicolor Fluorescent DNA Analysis. *Adv. Funct. Mater.* **2010**, 20, 453-459.

(36) Ueno, Y.; Furukawa, K.; Matsuo, K.; Inoue, S.; Hayashi, K.; Hibino, H., Molecular Design for Enhanced Sensitivity of a FRET Aptasensor Built on the Graphene Oxide Surface. *Chem. Commun.* **2013**, 49, 10346-10348.

(37) Antony, J.; Grimme, S., Structures and Interaction Energies of Stacked Graphene-Nucleobase Complexes. *Phys. Chem. Chem. Phys.* **2008**, 10, 2722-2729.

(38) Varghese, N.; Mogera, U.; Govindaraj, A.; Das, A.; Maiti, P. K.; Sood, A. K.; Rao, C. N. R., Binding of DNA Nucleobases and Nucleosides with Graphene. *ChemPhysChem* **2009**, 10, 206-210.

(39) Tang, L. H.; Wang, Y.; Liu, Y.; Li, J. H., DNA-Directed Self-Assembly of Graphene Oxide with Applications to Ultrasensitive Oligonucleotide Assay. *ACS Nano* **2011**, 5, 3817-3822.

(40) Piao, Y.; Liu, F.; Seo, T. S., The Photoluminescent Graphene Oxide Serves as an Acceptor Rather than a Donor in the Fluorescence Resonance Energy Transfer Pair of Cy3.5-Graphene Oxide. *Chem. Commun.* **2011**, 47, 12149-12151.

(41) Lu, C.; Huang, Z.; Liu, B.; Liu, Y.; Ying, Y.; Liu, J., Poly-Cytosine DNA as a High-Affinity Ligand for Inorganic Nanomaterials. *Angew. Chem., Int. Ed.* **2017**, 56, 6208-6212.

(42) Dong, Y. C.; Yang, Z. Q.; Liu, D. S., DNA Nanotechnology Based on i-Motif Structures. *Acc. Chem. Res.* **2014**, 47, 1853-1860.

(43) Li, X.; Peng, Y.; Ren, J.; Qu, X., Carboxyl-Modified Single-Walled Carbon Nanotubes Selectively Induce Human Telomeric I-Motif Formation. *Proc. Natl. Acad. Sci. U.S.A.* **2006**, 103, 19658-19663.

(44) Peng, Y.; Wang, X.; Xiao, Y.; Feng, L.; Zhao, C.; Ren, J.; Qu, X., I-Motif Quadruplex DNA-Based Biosensor for Distinguishing Single- and Multiwalled Carbon Nanotubes. *J. Am. Chem. Soc.* **2009**, 131, 13813-13818.

(45) Jin, K. S.; Shin, S. R.; Ahn, B.; Jin, S.; Rho, Y.; Kim, H.; Kim, S. J.; Ree, M., Effect of $C_{60}$ Fullerene on the Duplex Formation of i-Motif DNA with Complementary DNA in Solution. *J. Phys. Chem. B* **2010**, 114, 4783-4788.

(46) Chen, X.; Zhou, X.; Han, T.; Wu, J.; Zhang, J.; Guo, S., Stabilization and Induction of Oligonucleotide i-Motif Structure Via Graphene Quantum Dots. *ACS Nano* **2013**, 7, 531-537.

(47) Kimura-Suda, H.; Petrovykh, D. Y.; Tarlov, M. J.; Whitman, L. J., Base-Dependent Competitive Adsorption of Single-Stranded DNA on Gold. *J. Am. Chem. Soc.* **2003**, 125, 9014-9015.

(48) Manna, A. K.; Pati, S. K., Theoretical Understanding of Single-Stranded DNA Assisted Dispersion of Graphene. *J. Mater. Chem. B* **2013**, 1, 91-100.

(49) Ranganathan, S. V.; Halvorsen, K.; Myers, C. A.; Robertson, N. M.; Yigit, M. V.; Chen, A. A., Complex Thermodynamic Behavior of Single-Stranded Nucleic Acid Adsorption to Graphene Surfaces. *Langmuir* **2016**, 32, 6028-6034.

(50) Park, J. S.; Na, H.-K.; Min, D.-H.; Kim, D.-E., Desorption of Single-Stranded Nucleic Acids from Graphene Oxide by Disruption of Hydrogen Bonding. *Analyst* **2013**, 138, 1745-1749.

For table of content graphics only